JOURNAL OF GEOPHYSICAL RESEARCH, VOL. 100, NO. A7, PAGES 12,251–12,260, JULY 1, 1995

Radial alignment simulation of solar wind streams observed by Pioneers 10 and 11 in 1974

V. J. Pizzo[1]

San Juan Capistrano Research Institute, San Juan Capistrano, California

D. S. Intriligator and G. L. Siscoe

Carmel Research Center, Santa Monica, California

Abstract. A particularly favorable radial lineup between spacecraft in Earth orbit and Pioneers 10 and 11 (near the ecliptic plane at ~5.5 AU and ~4.5 AU, respectively) occurred in mid-1974, when the solar corona was in a stable and well-defined warped-dipole configuration. The radial alignment study reported here differs from previous applications of the technique in two respects: (1) It is the first time a two-dimensional (2-D) MHD model has been tested over such a lengthy propagation interval; the 2-D capability is crucial for treatment of the nonradial shearing motions occurring across the stream interface. (2) The three-dimensional (3-D) structure observed in the white light corona at that time is related to the systematic patterns of nonradial flow deflections appearing at the Pioneer corotating interaction region (CIR) fronts. Comparison of predicted and observed flows for pairs of streams in two successive rotations reveals that when the parent coronal hole projects far across the solar equator in a predominantly north-south orientation (i.e., nearest the 2-D idealization), the mapping is accurate down to details of the flow structures. But where the spacecraft tracks along a latitudinal boundary of a hole or the associated stream front is inclined at a shallow angle to the equator, the numerical projections deviate systematically from the observations. Among the sources of error are 3-D dynamical interactions neglected in the model, differential rotation effects, and slow temporal evolution of the coronal structures. A characteristic pattern of north-south and east-west deflections indicative of the 3-D geometry appears across the CIRs, but these patterns evidently reflect primarily the local, as opposed to global, orientation of the 3-D stream fronts. Such patterns appear common in CIRs observed by Pioneer during this period. These findings thus hold special relevance for the analysis of Ulysses observations, since the present coronal configuration is similar to that of 1974.

Introduction

Radial alignments tests have long been used to investigate the accuracy and scope of applicability of various models of large-scale solar wind flow. The basis of the test is that the spacecraft farther out from the Sun samples the same material observed earlier by the nearer spacecraft, but in a dynamically evolved state that is relatively free of complications and ambiguities of interpretation usually introduced by latitudinal variations and secular changes in source conditions.

A particularly propitious constellation of spacecraft occurred in mid-1974, when the Pioneer 10 and 11 spacecraft (P10, P11) were separated by only a few degrees in heliographic latitude λ and longitude ℓ while spaced roughly 1 AU apart in heliocentric distance, r. For test purposes, the value of this period is greatly enhanced by the fact that around day-of-year (DOY) 200–250 in 1974 the Earth was also well lined up with the Pioneer spacecraft (angular separation as seen from the Sun, $\lesssim 10°$), and that data coverage for the Pioneers and IMP satellites during this time was unusually complete. Moreover, the alignment took place very near solar minimum, when the solar corona is in its most stable and simply structured state, which corresponds best to the assumptions built into models of corotating flow structure. For all theses reasons, the flows of this time period have figured in a number of papers aimed at probing various aspects of interplanetary dynamics [e.g., *Burlaga et al.* 1990; *Siscoe and Intriligator*, 1993, 1994].

[1] Also at Space Environment Laboratory, National Oceanic and Atmospheric Administration, Boulder, Colorado

Paper number 95JA00328.
0148-0227/95/95JA-00328$05.00

Given the numerous instances of dynamical radial mapping studies already published [e.g., *Gosling et al.* 1976; *Dryer et al.* 1978; *Smith et al.* 1981; *Whang and Burlaga*, 1985, 1986], further application of the method may appear marginal. This paper differs from previous studies in two ways:

1. This is the first time that a two-dimensional (2-D) MHD model has been used to propagate the solutions over a baseline as long as 3.5–4.5 AU (the only other 2-D mapping [*Burlaga et al.*, 1985] spanned $\lesssim 1$ AU); all other studies have employed one-dimensional (1-D) HD or MHD models. Neglect of the nonradial flow is especially debilitating for simulations at heliocentric distances $r \lesssim 5$–10 AU, where the stream front interaction is primarily a shear flow, often with strong components in both transverse directions [*Pizzo*, 1991]. A 1-D (radial interaction only) model will thus overestimate greatly the compression in a corotating interaction region (CIR) and can lead to spurious shock formation in the vicinity of the stream interface, by virtue of the strong speed gradients occurring there. (The "extra" shock pair at the leading edge of the 1-D CIR simulation in Figure 6 of *Gosling et al.* [1976] and the similar structures appearing in Figure 4 of *Whang and Burlaga* [1985] are good examples of this phenomenon.)

2. The results of the simulations are related to the three-dimensional (3-D) topology of the stream structure via white light observations of the coronal configuration and by analysis of the nonradial flow deflections associated with the CIRs.

Additionally, since the coronal configuration in 1974 was not unlike that being encountered in the Ulysses primary mission, reconsideration of the near-ecliptic Pioneer observations from a global perspective provides a useful complement to the current high-latitude survey.

Data

The interplanetary input data consist of hourly averages of plasma and magnetic field data collected by the Earth-orbiting IMP spacecraft, obtained from the National Space Science Data Center (NSSDC). Several important gaps in the NSSDC plasma data set were bridged with unpublished observations taken by the Los Alamos National Laboratory experiments aboard IMP 6 and 7. The reference data for the output are provided by the Ames Research Center plasma analyzer and Jet Propulsion Laboratory magnetometer instrumentation on P10 and P11, also in hourly average form. Vector data were transformed to the heliographic (Carrington) coordinate system to facilitate comparison with the simulations. Mauna Loa Solar Observatory K coronameter maps serve as an indicator of the global solar wind structure for the two Carrington rotations (1617 and 1618) of interest.

A steady, well-defined stream structure characteristic of solar wind in the ecliptic near solar minimum is depicted in Figure 1. Here the solid line represents 1-AU IMP measurements of solar wind speed, while the dots show the P10 and P11 observations at ~5.6 and ~4.5 AU, respectively, over the course of two solar rotations. Two large streams, one relatively narrow, steep-fronted and fast (A), the other more broad, rounded in profile, and somewhat slower at 1 AU (B), recur in each data set. (Subscripted symbols A_1, A_2, refer to successive recurrences.) Considerable evolution between IMP and P11, P10 is evident, with stream A being more eroded than stream B by dynamical interactions in transit to the Pioneer spacecraft. Forward/reverse shock pairs have formed in each case, and the profiles of the other flow parameters (flow deflections, thermodynamic and magnetic quantities, shown later) undergo more than enough evolution to provide suitable criteria for the radial alignment test. (IMP plasma and field parameters for this period may be viewed in Figure 5 of *Burlaga et al.* [1990]; see their streams C and D.)

Model

The numerical MHD model is the same as the one used in a previous radial alignment study [*Burlaga et al.*, 1985], a 2-D version of the 3-D global model thoroughly described by *Pizzo*, [1982]. The essentials are that IMP hourly averages of five bulk flow parameters [the radial and azimuthal (east-west) components of velocity, V_r, V_ϕ; the proton number density, n; the gas pressure, P (taken as $P = 2nkT$, where k is the Boltzmann constant and T is the observed ion temperature); and the radial magnetic field, B_r (computed from the observed field intensity, B, and V_r, V_ϕ, by means of the frozen-in condition)] are fed into the model at 1 AU and integrated outward by means of the 2-D MHD equations expressing conservation of mass, total

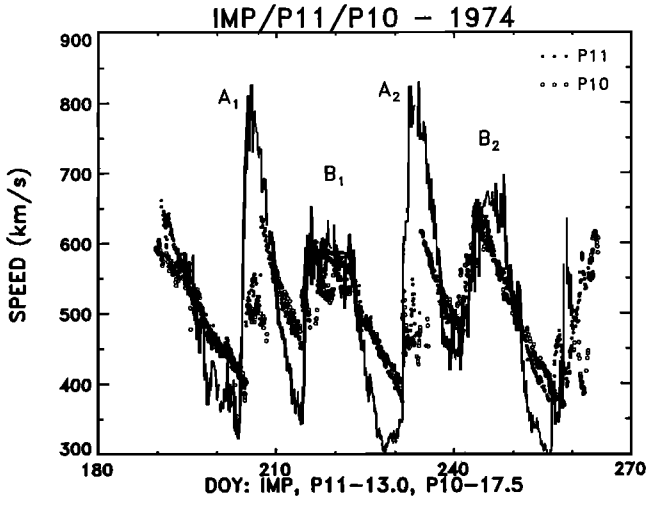

Figure 1. Two full rotations' worth of solar wind speed data from IMP and Pioneer 10 and 11 spacecraft during the latter half of 1974. The Pioneer data have been shifted by the indicated number of days to line up the plots. Stream A comes from the northern hemisphere of the Sun, and stream B from the south (see Figure 3). The two apparitions of the stream pair correspond to Carrington rotations 1617 and 1618.

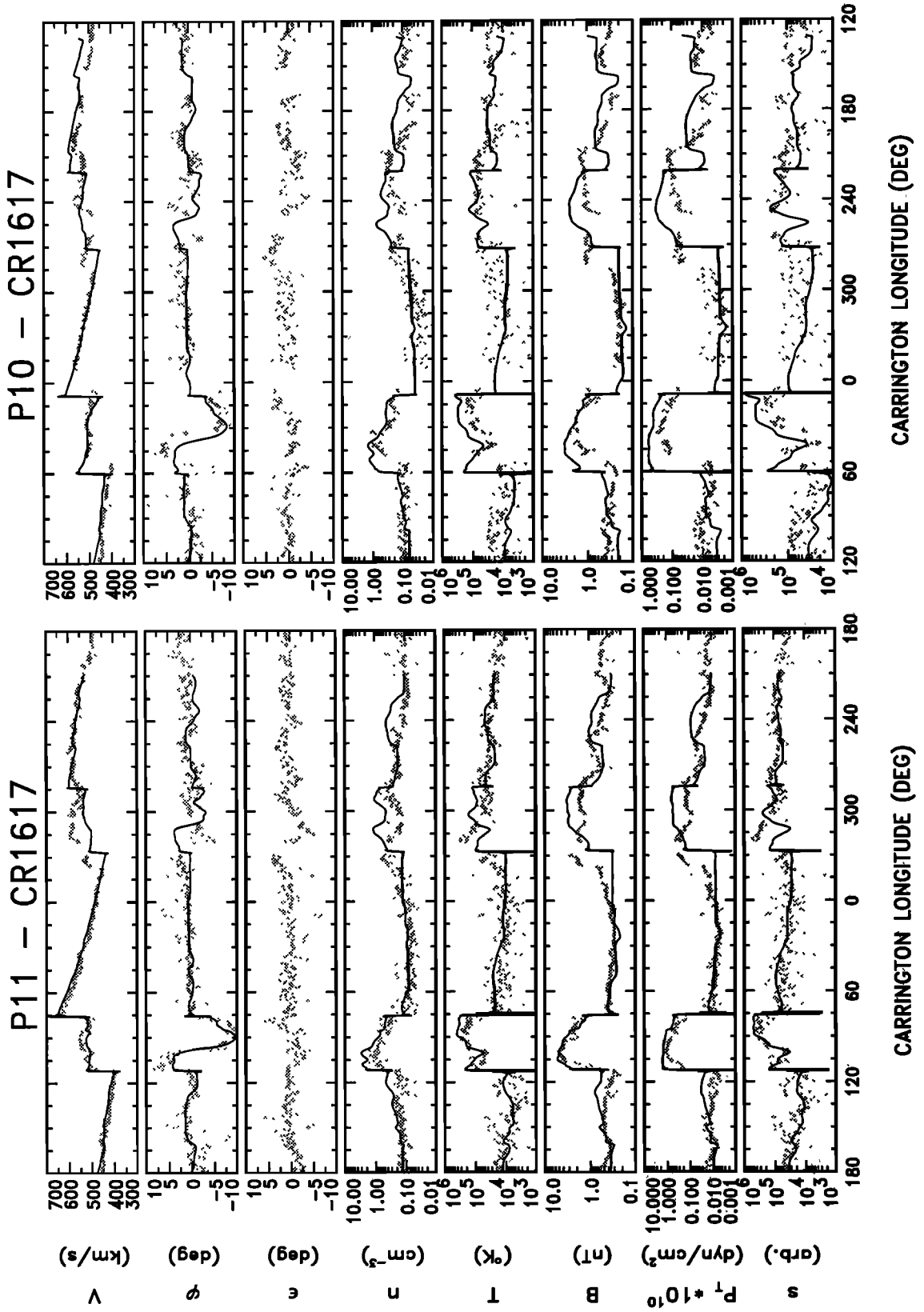

Figure 2. An overlay of the 2-D simulation predictions (line) and the Pioneer observations (dots) for CR1617. From top, the panels depict solar wind speed, the east-west flow angle, the north-south flow angle, proton number density, temperature, magnetic field strength, total (gas plus magnetic) pressure, and argument of the entropy. P11 was at this time at 4.43 AU, and P10 at 5.67 AU; both were within 2° of the ecliptic plane.

energy, momentum, and magnetic flux. The internal energy is described by a polytropic law, with the index $\gamma = 1.5$. This value is taken because it matches the entropy variations for these streams better than the usual 5/3 value [*Siscoe and Intriligator*, 1994], and it is consistent with the empirical mean solar wind value [*Totten et al.*, 1995]; using $\gamma = 5/3$ does not change the results appreciably. The thermodynamic treatment is limited by the lack of thermal electron data for comparison and by the use of the single-fluid formulation in the simulation. Residual data gaps (none significant) are filled in with linear interpolation. The hourly cadence of data corresponds to an angular resolution of ~0.55° in ℓ. A second-order filtering algorithm is used to keep the shocks numerically manageable, but the large-scale results reported here are not sensitive to this artifice.

Computational Results

The IMP input flow conditions are propagated out to the positions of the Pioneer spacecraft, for comparison with the observed data. Results for each solar rotation are discussed separately below.

Carrington Rotation 1617

The two halves of Figure 2 show the predictions of the simulation (line) overlaid on the observed Pioneer spacecraft data (dots). Both data strings are carefully registered to Carrington longitude to facilitate comparison of arrival times, in addition to overall waveform. The left half of the figure depicts the outcome at P11 ($r = 4.33$ AU), and the right half at P10 ($r = 5.66$ AU). From the top, the individual panels present the flow speed, the east-west flow deflection, the north-south flow deflection, the number density, the ion (single-fluid) temperature, the magnetic field intensity, the total pressure (gas plus magnetic), and the argument of the entropy ($= T/n^{\gamma-1}$). (There is no model prediction for ϵ, the north-south flow deflection, but we shall refer back to these observations later.)

The most obvious property of both plots is that while the simulation predicts two streams of the appropriate amplitude and breadth, stream A_1 matches the observations down to fine details, whereas the appearance of stream B_1 is delayed significantly in the simulation (i.e., it is shifted to the right with respect to the observed stream) and the parameter variations generally deviate further from the observed profiles. The correspondence for the nearer P11 is understandably better than that for the more distant P10, but the discrepancy with stream B_1 is substantial.

This latter point is underscored by the fact that because the flow is highly superalfvenic, the dynamics are strongly momentum dominated; on this basis alone we expect to model flow speeds more accurately than thermodynamics. Indeed, we here find the prediction for stream A_1 at P11 is good to about a half degree in longitude, comparable to the resolution of the computational mesh. On the other hand, the use of the polytropic description and the single-fluid formulation lower our expectations for the thermodynamic comparison. In addition, absolute instrumental calibrations in n and T among the various spacecraft are difficult to reconcile fully [e.g., *King*, 1977], contributing further to uncertainties in the radial mapping test.

Carrington Rotation 1618

Figure 3 presents the results of the simulation for the following Carrington rotation (CR) in the format of Figure 2. By this time, P11 had moved out to $r \sim 4.56$ AU, and P10 to $r \sim 5.79$ AU. Although the alignment with Earth was slightly better during CR1618 than in CR1617 and the input profiles look superficially the same, the comparison with the observations shows a dramatic reversal in "goodness of fit." That is, stream A_2 now exhibits major discrepancies with the observations, whereas the profiles for stream B_2 match much more closely. Although the flow variations about the interface of stream A_2 (the region marked by the strong east-west flow shift) are reasonably well modeled, this CIR appears grossly overcompressed and overexpanded, with the shock strengths and parameter jumps at the borders of the structure being greatly overestimated. Indeed, all the thermodynamic and magnetic parameters are unduly elevated throughout the body of the CIR; the error is so large and pervasive that it cannot be dismissed as a local inaccuracy at the shock fronts.

The fit to stream B_2, on the other hand, is much better. Although there is a noticeable translation of the simulated stream to the left, the overall waveform of the variations shows good correspondence with the observations. The speed profile at P11 is less evolved than in CR 1617: it is steepened but not saw-toothed, and while a reverse shock is clearly identifiable in the data, a forward shock is not. Both observation and simulation agree that the reverse shock becomes quite prominent at P10, while the forward shock is still in the process of forming.

It is worth stressing that the problem with stream A_2 is not due to data gaps or the method used to fill them. A major (~1 day) gap in B occurring near the front of the stream was treated in several different ways (linear interpolation, setting the missing data points to mean values, and so on), all with little influence on the result. Likewise, filling a gap in V_ϕ in the NSSDC data set with IMP 7 observations produced minimal change in the predicted flow profiles. Hence the source of the error does not lie in the details of the calculation, but rather stems from a major breakdown in the assumptions.

Relation to Coronal Structure

The two most questionable assumptions underlying the simulation concern the geometry and temporal variation. Although it would be easy to ascribe the errant predictions for B_1 and A_2 to nonstationarity, the data are sufficiently sparse that no quantitative assessments can be made. Hence a more fruitful course is to de-

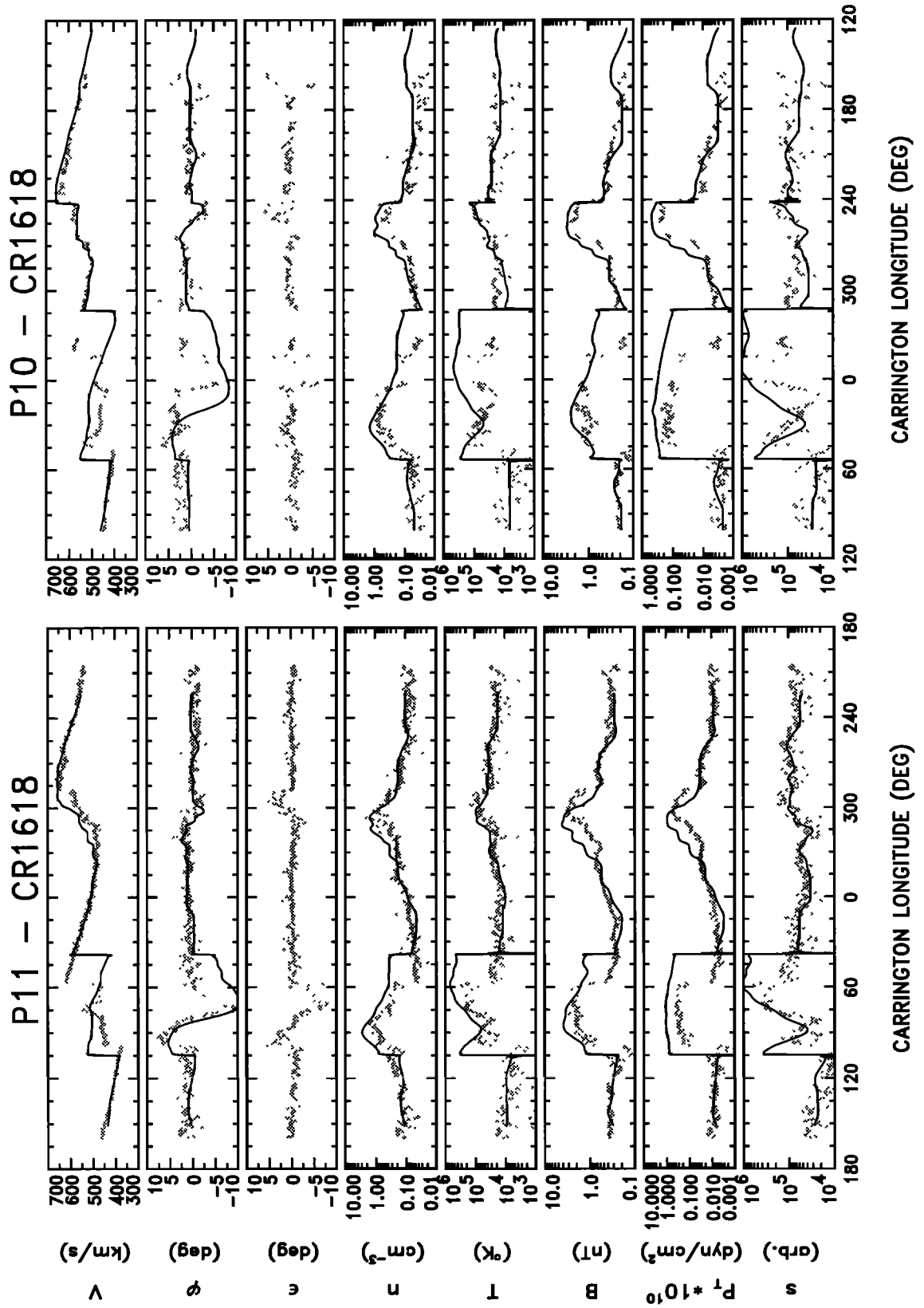

Figure 3. Same as Figure 2, but for the succeeding rotation, CR1618.

termine how much of the deviation may be attributed to the 3-D geometry of the flow. Here the Mauna Loa coronal maps provide an impression of the global configuration of the solar wind, and we can draw upon latent information in the flow angle deflections across the CIRs to infer something of the local flow geometry.

Figure 4 presents latitude-longitude contour plots of coronal polarization brightness at $r = 1.5R_S$ for CR1617 (top) and CR1618 (bottom), as measured by the Mauna Loa Solar Observatory. The two coronal holes marked A and B in each plot are the source of the interplanetary solar wind streams of interest to this study. The heliospheric current sheet (HCS) is not indicated here, but it is usually generated by connecting the points of peak brightness in the plot. The heliographic latitude of Earth (which differs from that of P10, P11 by only ±1.6° at this time) was near 7°N.

Although the overall pattern is relatively stable, details of the contours outlining the holes do change between the two rotations. In CR1618, A retreated significantly northward, while B expanded across the equator from the south. Note, too, that while hole A remained oriented nearly north-south and B continued to lie diagonally, the boundaries are not at all smooth and regular.

The geometries evident in Figure 4 must be interpreted cautiously. Each map is composited of individual line-of-sight averages taken over 14 days' time and refers to structure visible near one height in the corona. Both eclipse photographs and theoretical considerations suggest that substantial spatial evolution may occur outward from the nominal $1.5R_S$ height of the maps. Moreover, it is the configuration of the hole boundaries at unseen higher levels (perhaps as far out as the Alfven radius) that determines the geometry and orientation of the solar wind streams observed in interplanetary space. That is, the stream interface observed by interplanetary spacecraft as a relatively thin shear layer between fast and slow flows is directly related to the (presumably sharp) border between outflow from a hole and outflow associated with the streamer belt at coronal levels.

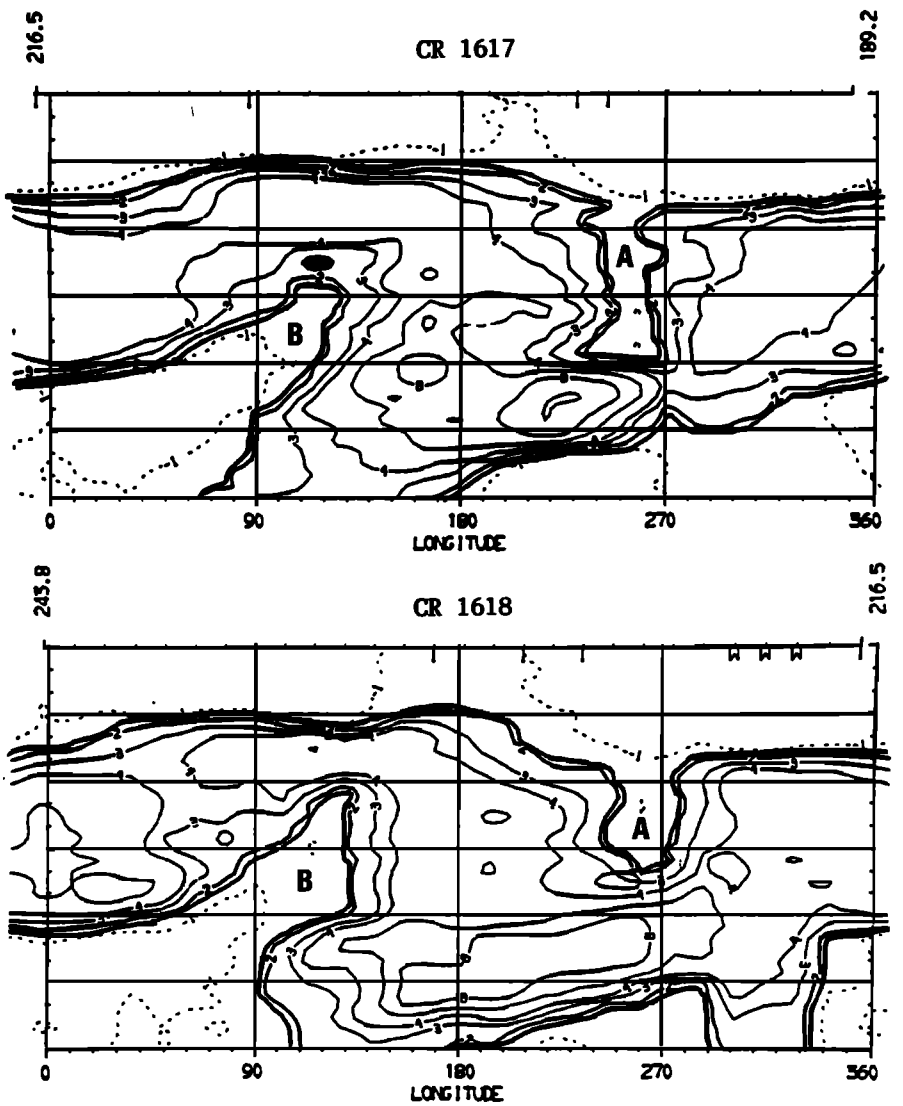

Figure 4. Map of coronal brightness, as observed by the Mauna Loa Solar Observatory. Contour levels are 1, 2, 3, 4, 6, 8, 10, 12 PB × 10^{-8}. This basic configuration persisted for many months, with minor changes from rotation to rotation.

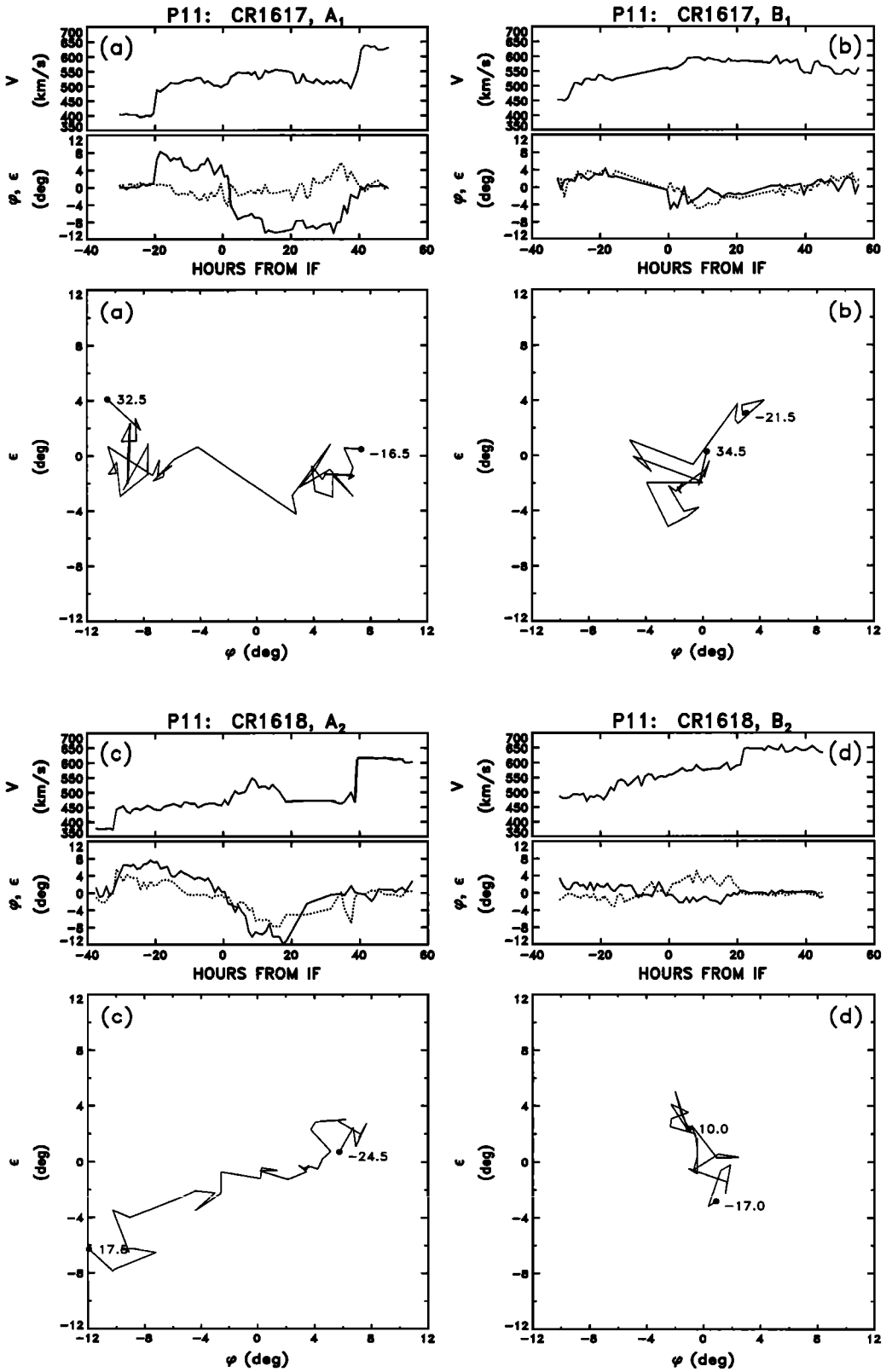

Figure 5. Details of interface structure at Pioneer 11 for both streams in the two rotations. In each segment of the figure, the top panel shows solar wind speed, the middle panel overlays the east-west (solid) and north-south (dots) flow deflections, and the bottom panel is a hodograph of the two nonradial components (begin and end times relative to interface "IF" passage indicated in hours).

The HCS itself is not necessarily coincident with the centroid of the streamer belt, and the streamer belt itself can vary considerably in cross-sectional width [e.g., *Winterhalter et al.* 1994]. Hence, although we expect the orientations of the HCS and the stream fronts to be similar in general, they need not be identical.

Nevertheless, several patterns do emerge. First, with regard to CR1617, we argue that the excellent predictions for stream A_1 stem from the fact that it so closely conforms to the 2-D idealization of the model: The coronal map shows the parent hole as oriented nearly north-south, and the track of the spacecraft runs right through the middle of it. The poor showing for stream B_1, on the other hand, may be attributed to the unfavorable location of the spacecraft toward the extreme northern boundary of the parent hole.

In CR1618, the spacecraft track much closer to the boundary of A_2 than in the previous rotation, but more nearly through the body of B_2. Since B_2 is broader in longitude than A_2 and its speed profile is also less steep (judging by the 1-AU observations), the dynamical interaction in B_2 should be more gradual. Hence the error caused through neglect of the full 3-D geometry in the model ought to be of less consequence for B_2 than for A_2, which explains in part why it is modeled more successfully.

However literally the plots of Figure 4 are taken, if the coronal geometry is invoked to explain the radial mapping discrepancies, it must account for two distinct types of errors. First, as in A_2, the CIR occurs at approximately the correct longitude, but the waveform of the variations is badly askew; second, as in B_2, the waveform replicates the observations quite well, but the CIR is bodily shifted in longitude. (Stream B_1 exhibits both types of error, but predominantly the shift.)

Were the coronal structure both absolutely stable and rigidly rotating, then the 3-D geometry could affect interplanetary CIRs in two ways: (1) the phase and waveform would depend on the latitude of observation simply because different spacecraft would be taking different cuts through a 3-D structure; and (2) the 3-D structure leads to 3-D dynamical transport, i.e., pressure gradients in the meridional direction drive north-south deflections of the flow, enhanced shearing relieves the compressional interactions, and so on. Since the Pioneer spacecraft differ from Earth in heliographic latitude by $\lesssim 1.6°$, it would appear that both kinds of mapping errors coming from the former source should be minimal. Both longitudinal shifts and change in waveform could arise from latter source, since the intensity of the interaction and propagation speeds can be affected.

Differential rotation in the corona can also contribute to the error, even if the hole structures themselves are relatively stable. The Carrington solar rotation rate of 25.38°/day (sidereal) is used in the computation, but it is well established that coronal structures can exhibit a range of rates (~25-26 days, sidereal), which vary with both latitude and time [*Fisher and Sime*, 1984; *Hoeksema and Scherrer*, 1987]; hemispheric differences are known as well. In particular, the former study suggests that the southern hemisphere (streams B_1, B_2) in 1974 tended to rotate slightly faster than the Carrington rate, which would cause the simulated streams to lag the observations. The maximum longitudinal shift introduced by this mechanism can be estimated from the fractional variation in rotation rates (~4%) operating over the net spiral offset between IMP and Pioneer (about 1/2 rotation), implying ~7° error. For stream B_1 in CR1617 this shift is in the right sense and large enough to account for much of the discrepancy; for CR1618, the magnitude is quite sufficient, but the sense is wrong. Note that differential rotation implies true time dependence; that is, there is no frame in which the entire pattern is steady, and the purely corotating formulation used in the simulations becomes increasingly deficient as the differential increases.

Finally, it is obvious that real coronal structures and the associated interplanetary flows are not absolutely stable. The magnitude of variation introduced by weak temporal evolution at the coronal source (and by differential rotation, as well) remains an unknown.

Flow Deflections

As stated above, if the global geometry in the corona is such as to generate strong 3-D interactions, then substantial north-south deflections should be observed in the resulting CIRs. It has previously been suggested [*Pizzo*, 1982, Figure 17 and associated discussion] that the large-scale spatial orientation of extended, sufficiently regular stream fronts can be inferred from the associated pattern of north-south and east-west flow deflections. These deflections can be of relatively large amplitude, with their phasing and magnitude being determined largely by the geometry of the flow at the coronal source (see also *Pizzo* [1991]). In particular, the relative amplitudes of the north-south deflection ϵ and the east-west deflection φ should be given by

$$\cot \iota \approx \epsilon/\varphi \tag{1}$$

where ι is the included angle between the stream front and the solar equator. (For tilted-dipole flow configurations, ι is closely related to, but not necessarily the same as, the dipole tilt angle.) This concept has proven useful in explaining large-scale systematic nonradial flow deflections in the outer heliosphere [*Pizzo*, 1994a] and, more recently, in elucidating the geometry of CIR structures observed by Ulysses well off the ecliptic plane [*Pizzo and Gosling*, 1994]. Encouraged by these results, we find it worthwhile to investigate how well the deflections observed by P10 and P11 conform to this notion.

Where the CIR can be modeled as a locally planar high-pressure ridge, (1) implies that a time sequence of the nonradial flow deflections plotted as ϵ versus φ should therefore form a straight line with slope $\cot \iota$. Flow deflections across the four CIRs observed by P11 in the two rotations of interest are shown in Figure 5. In each case, the top panel shows a segment of the speed

profile registered to the time of passage of the stream interface (hour = 0), and just below is an overlay of the associated east-west (solid) and north-south (dots) deflections; the square panel at bottom is a hodograph of the nonradial deflections, with start and end points as annotated (in hours, relative to interface passage).

For A_1 (Figure 5a), the flow deflections are predominantly east-west, consistent with the idea that the compression ridge of the CIR runs nearly north-south. For B_1, on the other hand, the amplitudes are smaller, and the progression of angle in the hodograph plot meanders about, so that a straight line fit to the track is questionable. Indeed, at P10 (not shown), the hodograph trajectory is rather more like a rotation, which is the pattern expected near the latitudinal boundary of a 3-D CIR structure (see panel 3 of Figure 17 of *Pizzo* [1982]).

In CR1618, the hodographs portray the clean linear trajectories characteristic of tilted, locally planar fronts. Figure 5c indicates that A_2 is inclined roughly 30° to the spin axis (i.e., the angle ι between the front and the equator is ~60°), as projected onto the latitude-longitude surface. (The full 3-D orientation of the front also depends upon the spiral wrapping of the front, as illustrated in Figure 2 of *Pizzo* [1991]. That is, the relation for $\cot \iota$ involves only two of the three flow components.) Stream B_2 is tilted even further poleward, the implied $\iota \approx 60°$. But there is an evident flaw in the theoretical scenario: Both streams are inclined the "wrong" way. That is, since A_2 is a northerly stream, we would expect the meridional component of the nonradial flow first to deflect southward at the front of the CIR, and then to swing back northward after passage of the interface; for the southerly stream B_2 we would expect the reverse sequence. Yet Figures 5c and 5d clearly show the opposite behavior.

This effect is real and is definitely not simply an error in coordinate specification; it has previously been noted that the sense of the meridional deflections in a few high-latitude CIRs observed by Ulysses also runs contrary to expectations [*Gosling et al.*, 1993]. We believe that the resolution of the dilemma lies in the fact that the flow deflections are indicative mainly of the local, as opposed to global, orientation of the stream front. The 3-D simulations offered to explain the Ulysses observations [*Pizzo and Gosling*, 1994] were predicated upon a highly idealized tilted-dipole flow, in which the slow flow band defining the magnetic equator was absolutely flat. Because of the inordinate smoothness of the input conditions, out to ~5 AU both northern and southern high-speed streams in this two-sector flow maintain a uniform pattern of north-south deflections all along each CIR. At greater heliocentric distances, however, 3-D interactions begin to corrugate the initially smooth CIR fronts, particularly at heliocentric latitudes lying within the extremes of the HCS band (see Figure 1 of *Pizzo* [1994b]), such that locally the north-south orientation can be opposite to the prevailing sense of the dipole tilt configuration.

Smaller-scale irregularities embedded in the flow at the source should greatly exacerbate this process. The HCS, for example, is known even at 1 AU to be considerably more corrugated on the large scale than coronal maps suggest [e.g., *Villante et al.*, 1979; *Gosling et al.*, 1981], and the tilts can differ appreciably (sometimes pointing in the opposite direction) from what is inferred from source surface projections [*Shodhan et al.*, 1994]. Hence it is not unreasonable to suppose that the entire slow flow band in which the HCS is embedded is also warped and irregular. We therefore conjecture that the situation with respect to north-south flow deflections may be analogous to that for the spiral field angle: At any time and place the field angle can wander all about, but in the mean it comes nearly to the Parker value. Likewise, the flow angles are subject to local fluctuations caused by small-scale roughness in the stream front structure, but they should, on average, reflect the large-scale orientation of the front. (Note that this applies preferentially to north-south deflections; east-west deflections are directly driven by the rotational interaction, and are thus far more constrained by global dynamics.)

Hence we tentatively conclude that although systematic north-south deflections in CIRs are indeed the signature of the 3-D geometry, they must be interpreted gingerly, especially near the ecliptic plane where the overall dynamic structure is complicated most by rotational effects.

Summary and Discussion

We have shown that in those circumstances where the model should work well (i.e., when the stream configuration best emulates an ideal steady, 2-D state) it does so, down to the details of various dynamical structures in the flow. Conversely, in those cases where it should not (i.e., where the 3-D aspects of the geometry are pronounced) it does not. Temporal variations undoubtedly contribute to inaccuracies in the performance of the model, but it is clear that 3-D effects played a significant, perhaps dominant, role in the case of the 1974 streams. A cursory perusal of the Pioneer record for this period reveals many instances of substantial north-south flow deflections accompanying CIR fronts, so 3-D effects may be expected to be the rule, rather than the exception, in CIR evolution.

Although the pattern of north-south flow deflections across a CIR front is indicative of the presence of 3-D structure, our results suggest that warps and folds in the flow structure may frustrate attempts to infer the general orientation on more than a local scale. The consistency of the deflections seen by Ulysses near the top of the streamer belt probably stems from the reduction in longitudinal variation in the corona at high latitudes; that is, the flow there is simpler and more uniform than it is near the ecliptic, which permits a more direct interpretation of the flow deflections. A statistical study of the relationship between the north-south flows in Pioneer CIRs and coronal source conditions is currently

under way. [A similar investigation of stream fronts in the inner heliosphere is also in progress; G. Lindsay, private communication, 1994].

This study lends strong credence to the view that the physical content of current multidimensional MHD models provides an entirely adequate description of interplanetary dynamical mechanisms on the large scale. In light of recent successes in simulating high-latitude CIR structure observed by Ulysses [*Pizzo and Gosling*, 1994], this conclusion would appear to extend to global aspects of the flow structure, at least insofar as corotating structures are concerned. Thus there is justification for taking confidence in predictions by such models of large-scale dynamical phenomena not readily accessible to in situ observation and for conducting further such simulations to study the evolution and merging of streams in the outer heliosphere. Whether multidimensional time-dependent structure can be modeled so faithfully remains to be proven, but continued investigation of 3-D processes manifest in the combination of Pioneer, Voyager, Ulysses, and other relevant data sets provides a sound basis for continued progress.

Acknowledgments. The work of V.J.P. (SJI contribution 0022) was conducted under the auspices of the San Juan Capistrano Research Institute and was supported by NASA grant NAG 2-752 in the Space Physics Division. He also expresses his gratitude to E. Hildner for continued support as a guest research at the Space Environment Laboratory. The work of D.S.I. and G.S. carried out at Carmel Research Center was supported by NASA/Ames Research Center under contract NAS 2-13692. NASA/Ames plasma data for this study were kindly provided by A. Barnes and P. Gazis, JPL magnetometer data were supplied by E. J. Smith, the IMP 6 and 7 data used to supplement the NSSDC compilation came from J. Gosling at LANL, and the MLSO coronagraph plots were made available by D. G. Sime.

The Editor thanks J. Feynman and another referee for their assistance in evaluating this paper.

References

Burlaga, L. F., V. J. Pizzo, A. Lazarus, and P. Gazis, Stream dynamics between 1 AU and 2 AU: A comparison of observations and theory, *J. Geophys. Res.*, *90*, 7377, 1985.

Burlaga, L. F., W. H. Mish, and Y. C. Whang, Coalescence of recurrent streams of different sizes and amplitudes, *J. Geophys. Res.*, *95*, 4247, 1990.

Dryer, M., Z. K. Smith, E. J. Smith, J. D. Mihalov, J. H. Wolfe, R. S. Steinolfson, and S. T. Wu, Dynamic MHD modeling of solar wind corotating stream interaction regions observed by Pioneer 10 and 11, *J. Geophys. Res.*, *83*, 4347, 1978.

Fisher, R., and D. G. Sime, Rotational characteristics fo the white-light solar corona: 1965-1983, *Astrophys. J.*, *287*, 959, 1984.

Gosling, J. T., A. J. Hundhausen, and S. J. Bame, Solar wind stream evolution at large heliocentric distances: Experimental demonstration and the test of a model, *J. Geophys. Res.*, *81*, 2111, 1976.

Gosling, J. T., G. Borrini, S. J. Bame, W. C. Feldman, and R. T. Hansen, Coronal streamers in the solar wind at 1 AU, *J. Geophys. Res.*, *86*, 5438, 1981.

Gosling, J. T., S. J. Bame, D. J. McComas, J. L. Phillips, V. J. Pizzo, B. E. Goldstein, and M. Neugebauer, Latitudinal variation of solar wind corotating stream interaction regions: Ulysses, *Geophys. Res. Lett.*, *20*, 2789, 1993.

Hoeksema, J. T., and P. H. Scherrer, Rotation of the coronal magnetic field, *Astrophys. J.*, *318*, 428, 1987.

King, J., Interplanetary Medium Data Book, *Rep. NSSDC 77-04*, pp. 1-28, NASA, Goddard Space Flight Center, Greenbelt, Md., 1977.

Pizzo, V., A three-dimensional model of corotating streams in the solar wind, 3, Magnetohydrodynamic streams, *J. Geophys. Res.*, *87*, 4374, 1982.

Pizzo, V. J., The evolution of corotating stream fronts near the ecliptic plane in the inner solar system, 2, Three-dimensional tilted-dipole fronts, *J. Geophys. Res.*, *96*, 5405, 1991.

Pizzo, V. J., Global, quasi-steady dynamics of the distant solar wind, 1, Origins of north-south flows in the outer heliosphere, *J. Geophys. Res.*, *99*, 4173, 1994a.

Pizzo, V. J., Global, quasi-steady dynamics of the distant solar wind, 2, Deformation of the heliospheric current sheet, *J. Geophys. Res.*, *99*, 4185, 1994b.

Pizzo, V. J., and J. T. Gosling, 3-D simulation of high-latitude interaction regions: Comparison with Ulysses results, *Geophys. Res. Lett.*, *21*, 2063, 1994.

Shodhan, S., N. U. Crooker, W. J. Hughes, and G. L. Siscoe, Heliospheric current sheet inclinations predicted from source surface maps, *J. Geophys. Res.*, *99*, 2531, 1994.

Siscoe, G., and D. Intriligator, Three views of two giant streams: Aligned observations at 1 AU, 4.6 AU, and 5.9 AU, *Geophys. Res. Lett.*, *20*, 2267, 1993.

Siscoe, G., and D. Intriligator, Macroscale coherence of the heliospheric current sheet: Pioneers 10 and 11 comparisons, *Geophys. Res. Lett.*, *21*, 2075, 1994.

Smith, Z. K., M. Dryer, R. W. Fillius, E. J. Smith, and J. H. Wolfe, Compression of Jupiter's magnetosphere by the solar wind: Reexamination via MHD simulation of evolving corotating interaction regions, *J. Geophys. Res.*, *86*, 6773, 1981.

Totten, T. L., J. W. Freeman, and S. Arya, An empirical determination of the polytropic index for the free-streaming solar wind using Helios 1 data, *J. Geophys. Res.*, *100*, 13, 1995.

Villante, U., R. Bruno, F. Mariani, L. F. Burlaga, and N. F. Ness, The shape and location of the sector boundary surface in the inner solar system, *J. Geophys. Res.*, *84*, 6641, 1979.

Whang, Y. C., and L. F. Burlaga, Evolution and interaction of interplanetary shocks, *J. Geophys. Res.*, *90*, 10,765, 1985.

Whang, Y. C., and L. F. Burlaga, Coalescence of two merged interaction regions between 6.2 and 9.5 AU: September 1979 event, *J. Geophys. Res.*, *91*, 13,341, 1986.

Winterhalter, D., E. J. Smith, M. E. Burton, and N. Murphy, The heliospheric plasma sheet, *J. Geophys. Res.*, *99*, 6667, 1994.

V. J. Pizzo, R/E/SE, NOAA/SEL, 325 South Broadway, Boulder, CO 80303. (e-mail: vpizzo@sel.noaa.gov)

D. S. Intriligator, G. L. Siscoe, Carmel Research Center, P. O. Box 1732, Santa Monica, CA 90406. (e-mail: devriei@aol.com; siscoe@bu.edu)

(Received August 8, 1994; revised January 6, 1995; accepted January 24, 1995.)